8-2003

The Anisotropic Free Energy of the Lennard-Jones Crystal-Melt Interface

James R. Morris
Iowa State University

Xueyu Song
Iowa State University, xsong@iastate.edu

The Anisotropic Free Energy of the Lennard-Jones Crystal-Melt Interface

Abstract

We have calculated the free energy of the crystal-melt interface for the Lennard-Jones system as a function of crystal orientation, near zero pressure, by examining the roughness of the interface using molecular dynamic simulations. The anisotropy is weak, but can be accurately resolved using this approach due to the sensitivity of the fluctuations on the anisotropy. We find that the anisotropy can be described well using two parameters, based upon a low-order expansion satisfying cubic symmetry. The results are in good agreement with previous calculations of the free energies, based upon simulations used to calculate the reversible work required to create the interfaces. The weak anisotropy is also in reasonable agreement: The work here and the work of Davidchack and Laird [R. L. Davidchack and B. B. Laird, J. Chem. Phys. **118**, 7651 (2003)] both predict $\gamma 100 > \gamma 110 > \gamma 111$. The only discrepancy is that we find a smaller value for the difference $\gamma 100 - \gamma 111$ by an amount larger than the combined error bars.

The anisotropic free energy of the Lennard-Jones crystal-melt interface

James R. Morris and Xueyu Song

Articles you may be interested in

Direct calculation of the crystal–melt interfacial free energies for continuous potentials: Application to the Lennard-Jones system
J. Chem. Phys. **118**, 7651 (2003); 10.1063/1.1563248

Computer modeling of the liquid–vapor interface of an associating Lennard-Jones fluid
J. Chem. Phys. **118**, 329 (2003); 10.1063/1.1524158

Crystallization and melting in the Lennard-Jones system: Equilibration, relaxation, and long-time dynamics of the moving interface
J. Chem. Phys. **115**, 9434 (2001); 10.1063/1.1413972

Simulation of the third law free energies of face-centered-cubic and hexagonal-close-packed Lennard-Jones solids
J. Chem. Phys. **113**, 4320 (2000); 10.1063/1.1288185

Computer simulations of liquid/vapor interface in Lennard-Jones fluids: Some questions and answers
J. Chem. Phys. **111**, 8510 (1999); 10.1063/1.480192

The anisotropic free energy of the Lennard-Jones crystal-melt interface

James R. Morris
Metal and Ceramic Sciences Program, Ames Laboratory (U.S. Department of Energy), Iowa State University, Ames, Iowa 50011

Xueyu Song
Department of Chemistry, Iowa State University, Ames, Iowa 50011

We have calculated the free energy of the crystal-melt interface for the Lennard-Jones system as a function of crystal orientation, near zero pressure, by examining the roughness of the interface using molecular dynamic simulations. The anisotropy is weak, but can be accurately resolved using this approach due to the sensitivity of the fluctuations on the anisotropy. We find that the anisotropy can be described well using two parameters, based upon a low-order expansion satisfying cubic symmetry. The results are in good agreement with previous calculations of the free energies, based upon simulations used to calculate the reversible work required to create the interfaces. The weak anisotropy is also in reasonable agreement: The work here and the work of Davidchack and Laird [R. L. Davidchack and B. B. Laird, J. Chem. Phys. **118**, 7651 (2003)] both predict $\gamma_{100} > \gamma_{110} > \gamma_{111}$. The only discrepancy is that we find a smaller value for the difference $\gamma_{100} - \gamma_{111}$ by an amount larger than the combined error bars. © *2003 American Institute of Physics.*
[DOI: 10.1063/1.1591725]

I. INTRODUCTION

The free energy of the interface between a crystal and its melt is an important quantity, determining the nucleation rates and growth processes for undercooled liquids.[1–3] Within classical nucleation theory, the interfacial free energy creates the barrier to forming a nucleus. For dendrite growth processes, the free energy determines the conditions at the dendrite tip. In the latter process, the anisotropy of the interfacial free energy is also important, as it determines the stability of the dendrite growth.[4,5] This is true even for systems where the anisotropy is small, such as metallic systems where the anisotropy is on the order of 1%.

However, it is difficult to accurately determine the interfacial free energy, either experimentally or theoretically. Measurements of nucleation rates have provided some estimates,[1,2,6,7] utilizing classical nucleation theory, but presumably nucleation primarily occurs heterogeneously. More accurate techniques have been developed, examining the shape of the interface where it intersects a grain boundary. However, the number of grain boundary groove experiments are limited, and thus far they have not been used to determine the anisotropy of the free energy. Theoretically, the primary approach has been using density-functional theory; these have primarily focused on simple models (hard-sphere and Lennard-Jones systems) and have not led to consistent results.[8–11]

Calculations may also be made using atomistic simulations, in particular molecular dynamics. For the Lennard-Jones system, Broughton and Gilmer[12] used a "cleaving" approach, where a fictitious potential is used to create interfaces in bulk solid and liquid phases, and to then bring the interfaces into contact in a nearly reversible manner. The virtual work required to create the crystal-melt interfaces is then directly related to the interfacial free energy. This early work was unable to accurately determine the anisotropy, which is less than the error bars of their calculations. More recently, Davidchack and Laird[13] used a variation of this cleaving technique to calculate the interfacial free energy of a hard-sphere system, with reported accuracies sufficient to resolve the anisotropies. As expected, the anisotropy is small, on the order of several percent. They have subsequently applied this same technique to calculate the anisotropic free energy of the Lennard-Jones system.[14]

An alternate approach has been used and applied to a number of models of metals in recent years.[15–18] This approach utilizes simulations of the interface in equilibrium at the melting temperature, and examines the fluctuations in the height of the interface. For nearly isotropic systems, the interfaces are usually rough at the melting temperature. The magnitude of the fluctuations reflect the interfacial free energy; in particular, a low energy interface will have relatively small fluctuations, due to the cost both in forming additional interfacial energy and in deviating from the low-energy interface. Consider (for simplicity) a two-dimensional system: we may define the orientation of an interface by an angle θ, and the instantaneous deviation of the interface from its average position by a height $h(x)$ where x measures the distance along the interface. In Fourier space, the fluctuation associated with a wavenumber q should have an average square amplitude given by[19]

$$\langle |h(q)|^2 \rangle = \frac{k_B T}{\tilde{\gamma}(\theta) q^2}, \tag{1}$$

where θ gives the orientation of the interface, and the "interfacial stiffness" $\tilde{\gamma}(\theta)$ is related to the interfacial free energy $\gamma(\theta)$ by

$$\tilde{\gamma}(\theta) = \gamma(\theta) + \gamma''(\theta). \qquad (2)$$

For an isotropic system, the stiffness reduces back to the interfacial free energy. For an anisotropic system, however, the anisotropy of the stiffness is an order of magnitude larger than that of the free energy. Therefore, this fluctuation method is more sensitive to the anisotropy, allowing for an accurate determination of the full interfacial free energy and its dependence on crystal orientation.

In this paper, we present results using this method to analyze the interfacial free energy of the Lennard-Jones system, and compare with previous calculations. In particular, the recent results of Davidchack and Laird[14] provide a sensitive test of this method. As we shall demonstrate, our results are in close agreement with these previous calculations, validating the approach. Discrepancies are small, showing up mostly in the differences in free energies between different orientations. As this technique is quite sensitive to the anisotropy, we believe that our results are currently the most accurate determination of this quantity for this system.

II. THEORY AND APPROACH

To simulate the crystal-melt interface, we first simulate pure crystal and liquid phases separately, with identical cross sections. The crystal is oriented with the plane to be studied parallel to a simulation box side. The liquid and crystalline simulations are chosen to contain the same number of atoms, and each has the density appropriate for the bulk phase at the melting temperature. The systems are then equilibrated at the melting temperature. Note that the melting temperature can accurately be determined by coexistence simulations in essentially the same manner that we describe here.[20,21] In the simulations here, the average temperature and pressure were found to be $T_m = 0.620\epsilon$ and $P = -0.01\epsilon/\sigma^3$. The melting temperature is consistent with that found previously for this pressure.[21,22]

Subsequently, the systems are joined together, to create two crystal-melt interfaces that are initially flat. The system is briefly equilibrated (approximately 20 000 MD time steps) at the melting temperature. For the Lennard-Jones system, we chose a time step of $\Delta t = 0.0025\sqrt{m\sigma^2/\epsilon}$ where m sets the mass for the particle. We then scale velocity such that the *total* energy to a value halfway between the average energy of the bulk phases. In order to match pressures and temperatures between simulations of different interfaces, we ensure that the "production" runs all occur at the same total density and energy. An equilibration run is then performed at constant energy and volume; for the current work, this run was 500 000 MD time steps. The system was then run for two million time steps for data collection.

A snapshot of one such simulation is shown in Fig. 1. As can be seen, the system is chosen to be narrow in one direction (on the order of four lattice spacings), so that the height fluctuations will be essentially functions of only one direction. Thus, the results for the interfacial stiffness are not only a function of crystal orientation, but also the chosen "short" direction. This is implicit in Eq. (2) where the angle θ is
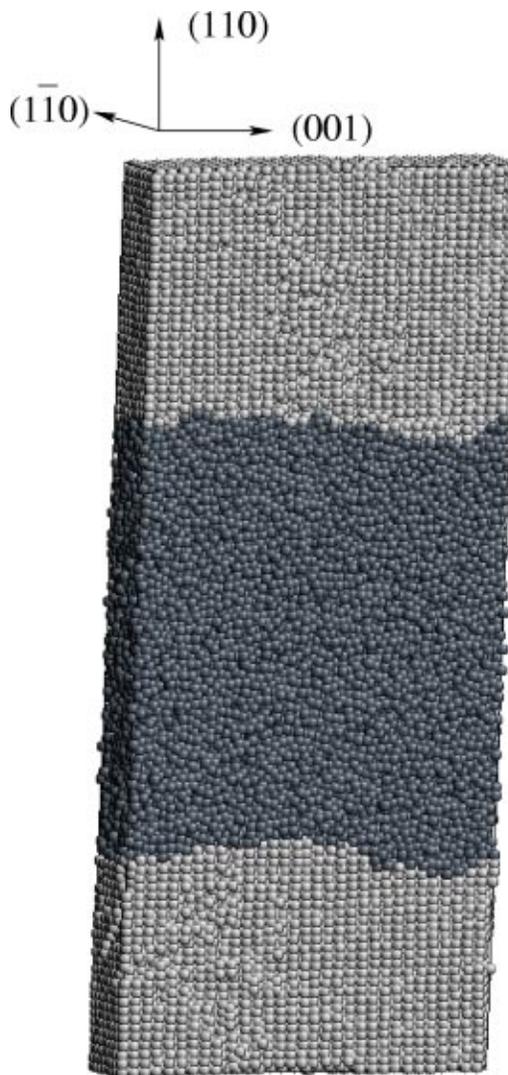

FIG. 1. A snapshot of the system with two (110) interfaces. Light atoms have a large value of local FCC order, while dark atoms have small values. The order parameter clearly separates the ordered solid region from the disordered, liquid region. The axes on top indicate the crystallographic directions. In the $[1\bar{1}0]$ direction (normal to the figure), the periodic repeat distance is significantly shorter than in the other directions.

measured about some axis. Six different crystal simulations were performed; these geometries are summarized in Table II.

During the runs, atomic positions were stored every 1000 time steps. Rather than store instantaneous configurations, the positions were averaged over 200 time steps. This averaging time is short compared with typical diffusion times in the liquid, but the resultant average atomic configuration is easier to analyze than an instantaneous configuration due to the absence of some of the high frequency fluctuations. This is important for accurately extracting out the interface height.

For calculating the interfacial height for each of the simulations, we have followed the same approach as in Ref. 16, and do not present the details here. Briefly, an order parameter is calculated for each atom, dependent upon the geometry of the surrounding atoms. For atoms in the liquid, this order parameter is small, while the crystalline region has

TABLE I. Summary of the interfaces simulated, including the short direction in the simulation. Note that the notation is different from that used in Refs. 15, 17, and 18. We also show the equations for interfacial stiffness in terms of γ_0 and the anisotropy parameters defined by Eq. (3).

Interface	Short direction	Interfacial free energy	Interfacial stiffness
(100)	[001]	$\gamma_0(1 + \frac{2}{5}\epsilon_1 + \frac{4}{7}\epsilon_2)$	$\gamma_0(1 - \frac{18}{5}\epsilon_1 - \frac{80}{7}\epsilon_2)$
(110)	[001]	$\gamma_0(1 - \frac{1}{10}\epsilon_1 - \frac{13}{14}\epsilon_2)$	$\gamma_0(1 + \frac{39}{10}\epsilon_1 + \frac{155}{14}\epsilon_2)$
(210)	[001]	$\gamma_0(1 + \frac{2}{25}\epsilon_1 - \frac{68}{175}\epsilon_2)$	$\gamma_0(1 + \frac{6}{5}\epsilon_1 - \frac{274}{35}\epsilon_2)$
(110)	[1$\bar{1}$0]	$\gamma_0(1 - \frac{1}{10}\epsilon_1 - \frac{13}{14}\epsilon_2)$	$\gamma_0(1 - \frac{21}{10}\epsilon_1 + \frac{365}{14}\epsilon_2)$
(111)	[1$\bar{1}$0]	$\gamma_0(1 - \frac{4}{15}\epsilon_1 + \frac{64}{63}\epsilon_2)$	$\gamma_0(1 + \frac{12}{5}\epsilon_1 - \frac{1847}{63}\epsilon_2)$
(112)	[1$\bar{1}$0]	$\gamma_0(1 - \frac{29}{90}\epsilon_1 - \frac{47}{126}\epsilon_2)$	$\gamma_0(1 + \frac{19}{10}\epsilon_1 + \frac{1255}{126}\epsilon_2)$

a larger value. In Fig. 1, the atoms have been shaded according to their order parameter; the sharp difference between the disordered and crystalline regions is apparent. The interfacial atoms have intermediate values of the order parameter, and thus the atoms at the interface can be extracted and used to calculate the interfacial height. From these height functions at regular intervals during the simulations, we calculate the quantity $\langle |h_{\mathbf{q}}|^2 \rangle$ needed to find the stiffness utilizing Eq. (1). We also note that we have attempted to distinguish between the atoms in liquid and solid regions by their potential energy, but found that the fluctuations were too large for this to be effective.

As indicated in the Introduction, the interfacial stiffness $\tilde{\gamma}$ is expected to be more anisotropic than the interfacial free energy γ. For weak anisotropy, the anisotropic interfacial free energy can be represented by a low order expansion consistent with cubic symmetry. We use the form from Ref. 23 which allows us to directly compare with the results from Ref. 14, In terms of the normal $\mathbf{n} = (n_x, n_y, n_z)$ we write the free energy as

$$\tilde{\gamma}(\mathbf{n}) = \gamma_0 \left[1 + \epsilon_1 \left(\sum_i n_i^4 - \frac{3}{5} \right) \right.$$
$$\left. + \epsilon_2 \left(3\sum_i n_i^4 + n_1^2 n_2^2 n_3^2 - \frac{17}{7} \right) \right], \quad (3)$$

where only the first two anisotropy terms have been kept. From this equation, we can derive equations for the stiffnesses; these (and the equations for the free energies) are given in Table I for the simulated geometries. As can be seen in these equations, the prefactors for the anisotropy parameters ϵ_1 and ϵ_2 are larger for the stiffness than the free energy, demonstrating that the stiffness is significantly more anisotropic.

III. SIMULATIONS AND INTERFACIAL STIFFNESS CALCULATIONS

In Fig. 2, we show the calculated values of $\langle |h(q)|^2 \rangle$ for each of the geometries, found using the approach described in the previous section. Error bars indicate the root-mean-square fluctuations of the values. The long wavelength (small q) portion of each graph has been fit to the form $1/q^2$, as anticipated in Eq. (1) The fluctuations clearly follow this behavior at small q, indicating the roughness of the interfaces. At larger q, the values of $\langle |h(q)|^2 \rangle$ deviate from this; we find that the values in this region are sensitive to the details of the method of defining the height function, while the small q region is not. Thus, we conclude that the interfaces are indeed rough, and we calculate the stiffnesses using Eq. (1). These values are given in Table II along with the
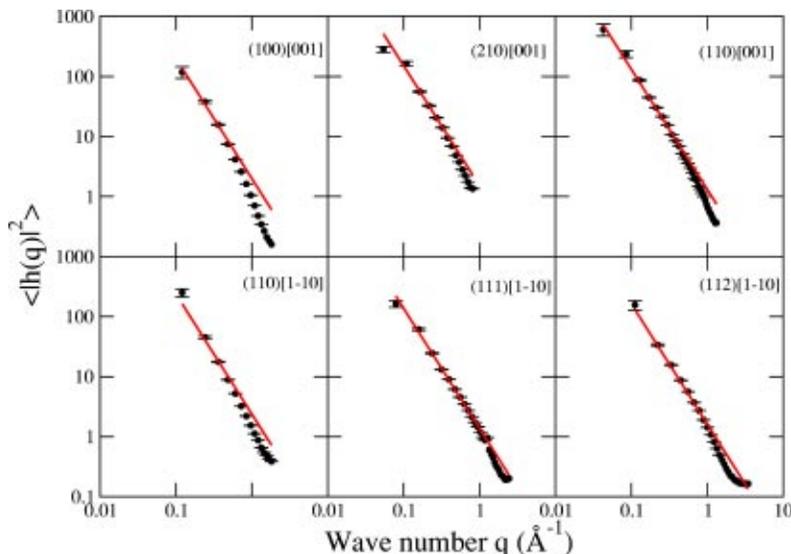

FIG. 2. Power spectrum of the height function, for different interfaces. The interfaces are specified both by the crystallography of the interface, as well as the "short" direction of the simulation (either [001] or [1$\bar{1}$0]). Note that Ref. 15 uses the "long" direction in their notation. Fits of the small q region to the form $k_B T / \tilde{\gamma} q^2$ are also shown.

TABLE II. Geometries and number of atoms used in interface simulations, and resultant interfacial stiffness $\tilde{\gamma}$. Also shown are the fitted interfacial stiffnesses, using the equations shown in Table I, with both one and two anisotropy parameters. Interfaces are labeled as in Table I. The geometry is shown with all lengths in units of σ, while all stiffnesses are in units of ϵ/σ^2.

Interface	Geometry	Number of atoms	Interface stiffness (height fluctuations)	Interface stiffness fit; $\epsilon_2=0$	Interface stiffness fitted both ϵ_1, ϵ_2
$(100)[001]$	$51.821\times55.131\times6.478$	16 384	0.31(5)	0.30	0.31
$(110)[001]$	$146.563\times58.475\times6.478$	49 152	0.47(7)	0.45	0.42
$(210)[001]$	$115.875\times61.639\times6.478$	40 960	0.41(4)	0.40	0.40
$(110)[1\bar{1}0]$	$51.821\times116.949\times9.161$	49 152	0.26(5)	0.32	0.27
$(111)[1\bar{1}0]$	$79.334\times59.681\times9.161$	38 400	0.45(4)	0.41	0.46
$(112)[1\bar{1}0]$	$56.098\times94.401\times9.161$	38 400	0.35(2)	0.40	0.38

appropriate error bars, indicating the uncertainty in the fit. As can be seen, the values for the stiffnesses range from $0.26\epsilon/\sigma^2$ to $0.47\epsilon/\sigma^2$, nearly a factor of 2. Thus, the stiffness does show significant anisotropy.

We now fit the stiffnesses to the equations given in Table I, to obtain the parameters γ_0, ϵ_1, and ϵ_2. To do this, we first note that the equations are linear in the combinations γ_0, $\gamma_0\epsilon_1$, and $\gamma_0\epsilon_2$. Thus, we treat these latter quantities as fitting parameters. We consider both the case where $\epsilon_2=0$, corresponding to keeping only the lowest order anisotropy term in Eq. (3), and the more general case where ϵ_2 is optimized. In the first case, we find the optimum fit to be (all in units of ϵ/σ^2) $\gamma_0=0.361(8)$, $\gamma_0\epsilon_1=0.022(3)$. In the latter case, we find $\gamma_0=0.362(8)$, $\gamma_0\epsilon_1=0.021(3)$, $\gamma_0\epsilon_2=-0.0017(5)$. Note that we can obtain the anisotropy terms more accurately than the average free energy γ_0, indicating that we can more accurately calculate the *difference* between free energies than absolute values. We also note that the parameters γ_0 and $\gamma_0\epsilon_1$ are insensitive to the fitting of $\gamma_0\epsilon_2$.

The calculated values of the stiffnesses from these parameters are given in Table II. While both forms give reasonable values, including the second anisotropy term noticeably improves the fit for stiffnesses calculated with a short direction of $[1\bar{1}0]$. This can be seen more directly in Fig. 3, where we show the anisotropic stiffness as a function of orientation in both the (100) and $(1\bar{1}0)$ plane. The data points from the simulation are shown, along with the curves calculated from the fitted parameters. As is clear in the figure, both forms of the fits are adequate to describe the results in the (100) plane, but the shape of the curve in the $(1\bar{1}0)$ plane is significantly affected by the inclusion of the second anisotropy term, shifting the maximum in the curve toward the (111) orientation. This second form is clearly more suitable for the simulation data, and closely reproduces all of the results.

We now compare with the results of Broughton and Gilmer[12] and of Davidchack and Laird.[14] In the former, the average interfacial free energy was found to be $\gamma_0=0.35(2)\epsilon/\sigma^2$; the error bars are larger than the observed differences between the values for the (100), $(1\bar{1}0)$, and (111) planes. In the latter, the error bars were much smaller, and they find $\gamma_0=0.360(2)\epsilon/\sigma^2$. These results are in excellent agreement with ours. In the latter work, the anisotropy parameters were also calculated, and they found the values $\epsilon_1=0.093(17)$ and $\epsilon_2=-0.011(4)$. Our determination of

these parameters is less accurate than the quantities $\gamma_0\epsilon_1$ and $\gamma_0\epsilon_2$, so we will compare these quantities instead. In this case, the results of Davidchack and Laird can be expressed as $\gamma_0\epsilon_1=0.033(6)\epsilon/\sigma^2$ and $\gamma_0\epsilon_2=-0.0040(14)\epsilon/\sigma^2$. While the parameters have the same sign as ours, they are both larger in magnitude, and are not consistent within the error bars of the two calculations.

To explore this further, we have calculated the stiffnesses from the parameters of Davidchack and Laird. We show this calculation in the polar plots of Fig. 3(b), along with our data and our two parameter fit. As can be seen, their results produce very good agreement with our simulation data except for the (110) plane with the $[1\bar{1}0]$ normal, and for the (111) interface. We also compare values for the interfacial free energies, in Table III, as well as values for the *difference* in the free energies. Again, our fitting produces more accurate
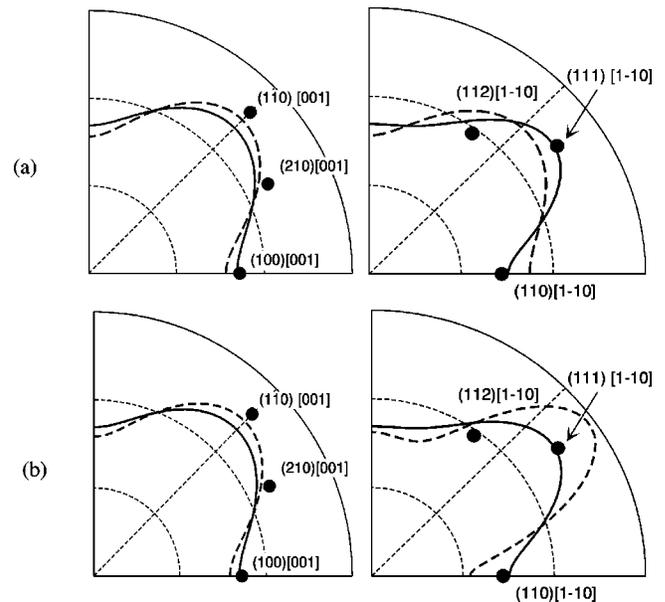

FIG. 3. Interfacial stiffnesses vs orientation, for interfaces with normals in the (001) plane and in the $(1\bar{1}0)$ plane. Large dots indicate results found from the simulations, while lines are calculated using Eq. (3). In (a), we show our one parameter expansion (dashed line) and our two parameter expansion (solid line) to demonstrate the improvement of the fit with the additional parameter. In (b), we compare our two parameter fit (solid line) with values calculated from the anisotropy parameters of Ref. 14. As can be seen, the latter results overestimate the interfacial stiffness of the (111) plane.

TABLE III. Interfacial free energies, calculated using the two-parameter anisotropy fit and from the equations given in Table I. We also compare with the results of Broughton and Gilmer (Ref. 12) and of Davidchack and Laird (Ref. 14), both for absolute interfacial free energies and for differences. All interfacial free energies are in units of ϵ/σ^2.

	Current work	Broughton and Gilmer	Davidchack and Laird
γ_{100}	0.369(8)	0.34(2)	0.371(3)
γ_{110}	0.361(8)	0.36(2)	0.360(3)
γ_{111}	0.355(8)	0.35(2)	0.347(3)
$\gamma_{100} - \gamma_{110}$	0.008(2)	0.02(3)	0.011(4)
$\gamma_{100} - \gamma_{111}$	0.016(2)	0.01(3)	0.024(4)

differences than absolute values, and this is reflected in the error estimates given in the table. We find $\gamma_{100} > \gamma_{110} > \gamma_{111}$, consistent with the results of Davidchack and Laird, but different than those of Broughton and Gilmer. Again, the error bars in the latter calculations make such a comparison not too significant. The value of $\gamma_{100} - \gamma_{110}$ from our calculation are within error bars of the value from Davidchack and Laird. However, the value of $\gamma_{100} - \gamma_{111}$ is smaller than that of Davidchack and Laird, by an amount larger than the combined error bars.

We can reconcile these discrepancies if we assume that the value of γ_{111} of Davidchack and Laird is too low, by an amount slightly greater than their error bars. As their results for the anisotropy are determined only by the three free energies, all of which are quite close, they are sensitive to small errors in any one of the calculations. Our calculations for the anisotropy parameters are in principle more accurate, for two reasons. First, our technique determines the parameters from quantities that are quite sensitive to the anisotropy, unlike the cleaving approach. Second, we are fitting our parameters to six geometries rather than three, and are therefore less sensitive to errors in any given result. This second point is not inherent in the approach, and further calculations using the cleaving approach with other planes would presumably give more accurate anisotropies. We also wish to note that the cleaving approach is clearly more accurate (in principle) for determining the average free energy γ_0, as it is a direct calculation of this quantity.

IV. DISCUSSION

We have simulated the fluctuations of different crystal-melt interfaces, and demonstrated that the fluctuations behave as expected for rough interfaces. From the fluctuations, we have calculated the anisotropic interfacial stiffness, and related this to the interfacial free energy $\gamma(\mathbf{n})$. The average interfacial stiffness was found to be $\gamma_0 = 0.362(8) \epsilon/\sigma^2$, in very good agreement with the value of $\gamma_0 = 0.360(2) \epsilon/\sigma^2$ found in recent calculations of the same quantity.[14] The latter calculations calculated the free energy by measuring the virtual work required to create the interfaces. Both techniques also predict that the interfacial free energies for the (100), (110), and (111) crystal interfaces satisfy $\gamma_{100} > \gamma_{110} > \gamma_{111}$. Both calculations show that the system is only weakly anisotropic. The fact that the two separate techniques predict es-

sentially the same γ_0 and also can discriminate the small differences between the different free energies for different orientations validates both techniques.

For the free energy difference $\gamma_{100} - \gamma_{110}$, both approaches essentially agree (within error bars) that this is 2–3 % of γ_0. However, there is a discrepancy in the value for $\gamma_{100} - \gamma_{111}$. As discussed in the results section, we believe that our value (approximately 4% of γ_0) is more accurate, as our approach is more sensitive to the *difference* between interfacial free energies than to the absolute values. This is a result of the fact that we measure quantities that depend sensitively upon the anisotropies of the free energy. In contrast, the virtual work approach directly determines the free energy, and therefore is more sensitive to the absolute value.

The same approach that we have used here has been used in calculating the anisotropy for models of Ni,[17] Al,[16] Au,[17] Ag,[17] and Ni–Cu.[18] The current work serves to validate this approach, by examining a more well-studied system. In this work and all of the above calculations, the results indicate that $\gamma_{100} > \gamma_{110} > \gamma_{111}$. Interestingly, however, the hard-sphere results indicate that $\gamma_{110} > \gamma_{100} > \gamma_{111}$. Much of the understanding of liquid properties, including liquid interfaces, comes from hard-sphere systems; indeed, the value of γ_0 can be understood in terms of the interfacial entropy found from hard sphere results.[24] The fact that the ordering found in more realistic models is different from the hard sphere results raises questions as to the origin of this difference. Both the attractive portion of the potential and the form of the repulsive interaction may be of importance. We are currently exploring this issue.

ACKNOWLEDGMENTS

[1] D. Turnbull, J. Appl. Phys. **21**, 1022 (1950).
[2] D. Turnbull and R. E. Cech, J. Appl. Phys. **21**, 804 (1950).
[3] D. P. Woodruff, *The Solid-Liquid Interface* (Cambridge University Press, Cambridge, 1973).
[4] D. I. Meiron, Phys. Rev. A **33**, 2704 (1986).
[5] D. A. Kessler and H. Levine, Phys. Rev. B **33**, 7867 (1986).
[6] K. F. Kelton, Solid State Phys. **45**, 75 (1991).
[7] D. Holland-Moritz, J. Schroers, D. M. Herlach, B. Grushko, and K. Urban, Acta Mater. **46**, 1601 (1998).
[8] W. A. Curtin, Phys. Rev. Lett. **59**, 1228 (1987).
[9] W. A. Curtin, Phys. Rev. B **39**, 6775 (89).
[10] D. W. Marr and A. P. Gast, Phys. Rev. E **47**, 1212 (1993).
[11] R. Ohnesorge, H. Lowen, and H. Wagner, Phys. Rev. E **50**, 1994 (1994).
[12] J. Q. Broughton and G. H. Gilmer, J. Chem. Phys. **84**, 5759 (1986).
[13] R. L. Davidchack and B. B. Laird, Phys. Rev. Lett. **85**, 4751 (2000).
[14] R. L. Davidchack and B. B. Laird, J. Chem. Phys. **118**, 7651 (2003).

[15] J. J. Hoyt, M. Asta, and A. Karma, Phys. Rev. Lett. **86**, 5530 (2001).
[16] J. R. Morris, Phys. Rev. B **66**, 144104 (2002).
[17] J. J. Hoyt and M. Asta, Phys. Rev. B **65**, 214106 (2002).
[18] M. Asta, J. J. Hoyt, and A. Karma, Phys. Rev. B **66**, 100101(R) (2002).
[19] A. Karma, Phys. Rev. E **48**, 3441 (1993).

[20] J. R. Morris, C. Z. Wang, K. M. Ho, and C. T. Chan, Phys. Rev. B **49**, 3109 (1994).
[21] J. R. Morris and X. Song, J. Chem. Phys. **116**, 9352 (2002).
[22] R. Agrawal and D. A. Kofke, Mol. Phys. **85**, 43 (1995).
[23] W. R. Fehlner and S. H. Vosko, Can. J. Phys. **54**, 2159 (1976).
[24] B. B. Laird, J. Chem. Phys. **115**, 2887 (2001).